Interference-free tool path generation for the robotic polishing of blisks

Yuanming Wang
Huazhong University of Science and Technology
Jixiang Yang (jixiangyang@hust.edu.cn)
Huazhong University of Science and Technology
Dingwei Li
Huazhong University of Science and Technology
Han Ding
Huazhong University of Science and Technology

Research Article

Keywords: blisk, polishing, collision detection, collision avoidance, tool-position correction

Posted Date: April 16th, 2021

DOI: https://doi.org/10.21203/rs.3.rs-412342/v1

Version of Record: A version of this preprint was published at The International Journal of Advanced Manufacturing Technology on August 6th, 2021. See the published version at https://doi.org/10.1007/s00170-021-07698-9.

Interference-free tool path generation for the robotic polishing of blisks

Yuanming Wang, Jixiang Yang*, Dingwei Li, Han Ding

School of Mechanical Science and Engineering, State Key Laboratory of Digital Manufacturing Equipments and Technology, Huazhong University of Science and Technology, Wuhan, 430074, P.R. China.

Abstract

In the robotic polishing process, the tool and the blisk interfere easily because of the narrow operation space and seriously twisted curved surfaces. Algorithms are proposed to detect and avoid collisions with high efficiency and accuracy. First, the curved surface of the blade is discretized into a set of points, and the collision detection between the tool and the blisk is converted into the calculation of distances between the tool and points on blade surface. Then, the tool axial vector is adjusted with the minimum rotation angle to avoid collision, which reduces the impact on surface profile accuracy after changing the tool postures. The machining quality is finally guaranteed by con-trolling the material removal depth of the polishing process. The proposed method realizes the collision detection and interference avoidance of the blisk polishing effectively, while it also ensures the surface quality of workpiece when adjusting the tool posture. Simulation and experiments are carried out to verify the feasibility and advantages of the proposed method.

Keywords: blisk; polishing; collision detection; collision avoidance; tool-position correction

1. Introduction

As the core part of aero engine, the surface quality of the blisk affects the service life and efficiency of the engine directly. Therefore, it is necessary to grind and polish the blisk after milling to improve the surface quality. Due to the complex geometric structure of the blisk, and its characteristics of distortion, deep and narrow flow channel [1], the tool interferes with the blisk easily during polishing, which makes the trajectory design of the blisk polishing compli-cated and challenging. The research of non-interference polishing technology for blisk is significant to improve the processing quality and promote the development of advanced manufacturing technology for aviation equipment [2,3].

Generally, the interferences between the tool and blisk are divided into two types: local interference and global in-terference [4]. Local interference is the interference between the cutting edge and the tool contact point on the ma-chined surface. It occurs when the tool radius is larger than the curvature radius at the contact point of the curved surface. When local interference occurs, the tool removes excessive materials near the contact point, which directly affects the quality of the machined surface. Global interference is the collision between the tool handle and the machining surface or other surfaces in the machining environment, which causes irreversible damage to the blisk and tool. A lot of scholars have conducted in-depth research on local interference, such as Ahmet [5], Lin [6], Fard [7], etc. Many methods based on differential geometry and curvature

* Corresponding author.

Email address: jixiangyang@hust.edu.cn (Jixiang Yang)

analysis have been successfully applied in detection and correction of local interference for complex surface processing. For global interference, finding the best pose where tools do not collide with the workpiece is a process of repeated inspections and corrections, which requires a large amount of calculation [8]. Therefore, the handling of global interference is much more complicated and difficult than local interference. This article focuses on the research of global interference of the blisk polishing.

In existing studies, different collision detection and avoidance algorithms have been proposed for processing interference problems of curved surface machining. Wang et al. [9] proposed a method of constructing collision-free regions without interference checking. This method searches the critical points between the holder and surface and calculates the corresponding critical tool vectors. Then, the critical tool vectors are mapped to a two-dimensional space and the collision-free regions are constructed. Ilushin et al. [10] proposed a collision detection method that uses space subdivision techniques and ray-tracing algorithms to derive a highly accurate polygon/surface–tool intersection algorithm. Ahmet et al. [5] proposed a method for determining the detection area and detection point based on the parameter area, and the interference is checked by calculating the maximum inclination of the connection between the tangential contact point and the detection point. Although this method is technically feasible, the calculation is large. Huang et al. [11] constructed a hierarchical OBB bounding box for the tool, which used the separation axis theory to identify the interference point, and realized the collision avoidance by adjusting the parameters of the tool and the tool bounding box vector. However, it does not consider the effect of changing tool posture on the surface quality of the workpiece.

From the above, it can be seen that existing methods of global interference detection and collision avoidance for curved surface do have contribution to check and avoid collision in order to achieve continuous and safe machining. However, very few methods consider the influence of the tool posture changes on the surface quality of the blisk. This paper proposes a method for generating a non-interference tool path by changing the tool axial vector to a safe position with the minimum rotation angle in the plane where the maximum interference is located, which ensures the machining quality by controlling the material removal depth of the polishing.

2. Collision detection method

Path planning methods for complex curved surfaces include isoparametric curve method [12], section plane method [13,14], constant scallop-height method [15] and projection method [16], etc. The collision detection and avoidance methods in this article are not limited to the initial path planning method, i.e., different path planning method can be selected according to needs. This paper uses the isoparametric method to generate the initial tool path of the blade. Initial tool postures $\{CL\}_{n=1}^{N}$ in the workpiece coordinate system are

$$CL = [p_x, p_y, p_z, n_x, n_y, n_z, t_x, t_y, t_z] \tag{1}$$

where $\boldsymbol{P}=\left[p_x, p_y, p_z\right]$ is the tool position in the workpiece coordinate system, $\boldsymbol{N}=\left[n_x, n_y, n_z\right]$ is the unit normal vector of the tool contact point, and $\boldsymbol{T}=\left[t_x, t_y, t_z\right]$ is the unit vector of the tool axis.

The diagram of blisk polishing is shown as Fig 1.

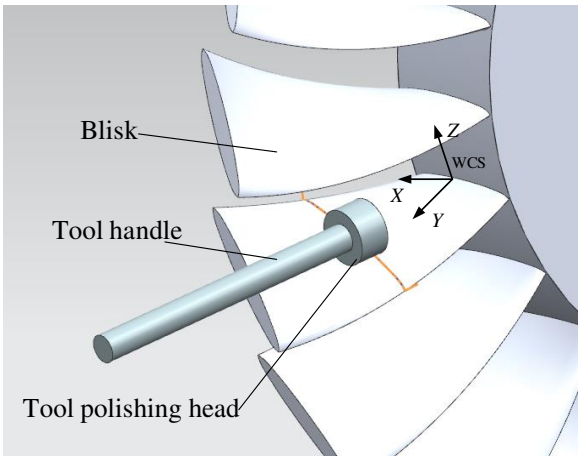

Fig 1 The diagram of blisk polishing

2.1 Discretization of blade surface

The collision detection between the tool and the blisk is an essential problem of judging whether the two sets of curved surfaces intersect. However, the calculation of collision between the surfaces is less effective and more difficult. The polishing tool is a standard cylinder, if the surface is discretized into a point set, the collision detection between the tool and the blisk is transferred to calculate the distance from the discrete point to the tool axis, which will improve the calculation efficiency.

When processing a certain blade surface, the tool will only interfere with two adjacent surfaces of the same flow channel, so only the two surfaces need to be discretized. B-spline surface is adopted to construct the blade surface, which is defined as

$$\boldsymbol{S}(u,v) = \sum_{i=0}^{m}\sum_{j=0}^{n}\boldsymbol{P}_{i,j}\boldsymbol{N}_{i,k}(u)\boldsymbol{N}_{j,l}(v) \tag{2}$$

In Eq. (2), $\boldsymbol{P}_{i,j}(i=0,1,\cdots\cdots m, j=0,1,\cdots\cdots n)$ is the control vertexes, $\boldsymbol{N}_{i,k}(u)$ and $\boldsymbol{N}_{j,l}(v)$ are the k-th and l-th B-spline basis functions defined along the u-direction and v-direction node vector respectively, where u and v are parameters of the surface.

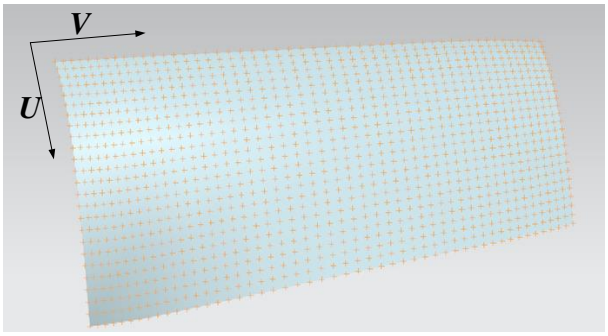

Fig 2 Isometric discretization of blade surface

As shown in Fig 2, by setting $\Delta u = \Delta v$, the blade surface is uniformly discretized into a set of points along the u, v isoparameters. The coordinates of the discrete point $\boldsymbol{F_i} = [x, y, z]$ corresponding to parameter (u, v) are obtained by Eq. (2).

2.2 Simplification of discrete points

In theory, the higher resolution the surfaces are discretized, the higher accuracy the collision detection can reach. However, as the discrete resolution increases, the number of discrete points will increase. If collision detection is performed on all discrete points, the calculation load will be heavy. In order to reduce the calculation burden, it is necessary to exclude discrete points that are impossible to interfere with the tool, in order to reduce the number of discrete points for collision detection.

As shown in Fig.1, the local workpiece coordinate system is established on the polishing blade. The tool handle is projected to the surfaces of two blades along the negative and positive directions of the *Z* axis in the workpiece coordinate system. Only discrete points located inside the tool handle projection may interfere with the tool.

As shown in Fig 3, the tool is projected to the surface of the polishing blade along the negative direction of the Z axis.

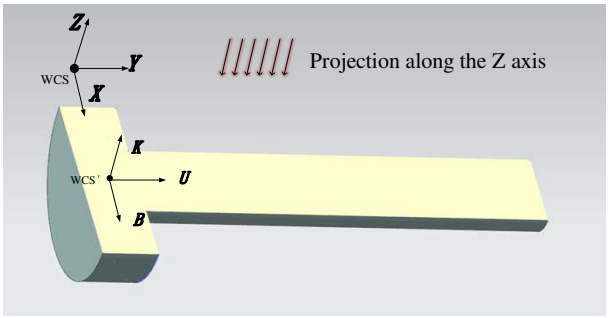

Fig 3 The tool is projected along the negative Z axis

$$\boldsymbol{U} = [u_x \quad u_y \quad u_z] = \left[\frac{t_x}{\sqrt{t_x^2+t_y^2}} \quad \frac{t_y}{\sqrt{t_x^2+t_y^2}} \quad 0 \right]$$

$$\boldsymbol{B} = [b_x \quad b_y \quad b_z] = \boldsymbol{U} \times \boldsymbol{K} \tag{3}$$

where $\boldsymbol{U}$ is the projected unit vector of the tool axis vector $\boldsymbol{T}$ on the *XOY* plane of the workpiece coordinate system, and $\boldsymbol{K}$ is the unit vector along the positive *Z* axis of the workpiece coordinate system.

In order to judge whether the discrete points are in the projection of the tool handle, temporary coordinate system WCS' is created whose origin is the tool position point and the coordinate axis directions are the vectors of $\boldsymbol{B}$, $\boldsymbol{U}$, $\boldsymbol{K}$ respectively.

The transformation matrix from the workpiece coordinate system to the temporary coordinate system is

$$\boldsymbol{E} = \begin{bmatrix} b_x & u_x & 0 & p_x \\ b_y & u_y & 0 & p_y \\ b_z & u_z & 1 & p_z \\ 0 & 0 & 0 & 1 \end{bmatrix} \tag{4}$$

The coordinates $\boldsymbol{F}_i'=[x',y',z']$ of the discrete point in the temporary coordinate system is calculated as

$$\begin{bmatrix} \boldsymbol{F}_i'^{\mathrm{T}} \\ 1 \end{bmatrix} = \boldsymbol{E} \begin{bmatrix} \boldsymbol{F}_i^{\mathrm{T}} \\ 1 \end{bmatrix} \tag{5}$$

If the position of the discrete point $\boldsymbol{F}_i'$ satisfies

$$\begin{aligned} |x'| &\le R_2 \\ \frac{L_1}{2} \le y' &\le \frac{L_1}{2} + L_2 \end{aligned} \tag{6}$$

The point $\boldsymbol{F}_i'$ fall inside the projected section of the tool handle, where L_1 is the width of the polishing head, L_2 is the length of the tool handle, and R_2 is the radius of the tool handle.

Only the discrete points fall inside the projected section of the tool handle may cause collision. For the points that are not in the projected section of the tool handle, collision could not happen, and they are eliminated in the following collision detection task in order to reduce the calculation burden.

2.3 Collision detection

By comparing the shortest distance from the discrete point to the tool axis with the radius of the tool handle, it is judged whether the tool interferes with the machined surface of the blisk. The detection process repeats until all discrete points are traversed.

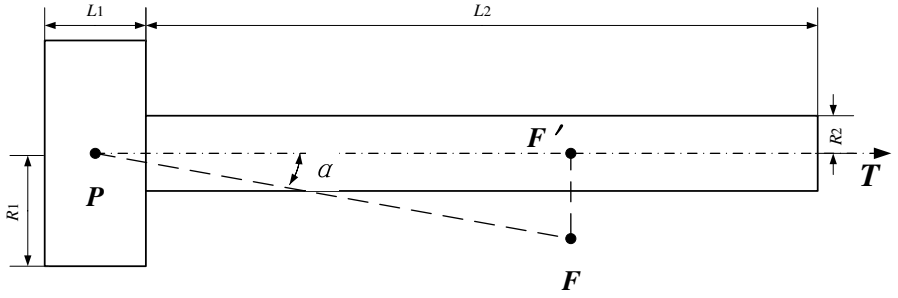

Fig 4 Discrete point and tool surface collision detection

As shown in Fig 4, $\boldsymbol{F}'$ is the projection of the discrete point $\boldsymbol{F}$ on the tool axis, and the shortest distance L from the discrete point to the tool axis is

$$L = \left\|\overrightarrow{\boldsymbol{FF}'}\right\| = \left\|\overrightarrow{\boldsymbol{PF}}\right\| \times \sin\alpha \tag{7}$$

where α is the angle between $\overrightarrow{\boldsymbol{PF}}$ and $\overrightarrow{\boldsymbol{PF}'}$, with

$$\alpha = \arccos \frac{\overrightarrow{\boldsymbol{PF}} \cdot \overrightarrow{\boldsymbol{PF}'}}{\left\|\overrightarrow{\boldsymbol{PF}}\right\| \times \left\|\overrightarrow{\boldsymbol{PF}'}\right\|} \tag{8}$$

By noticing as the safe distance between the tool and the blisk, if

$$L=R_2+ds \tag{9}$$

where ds is the safe distance between the tool and the blisk.

the tool and the blade collide at this tool position, where is the radius of the tool handle. As shown in Fig 5, the detection process repeats until all discrete points are traversed.

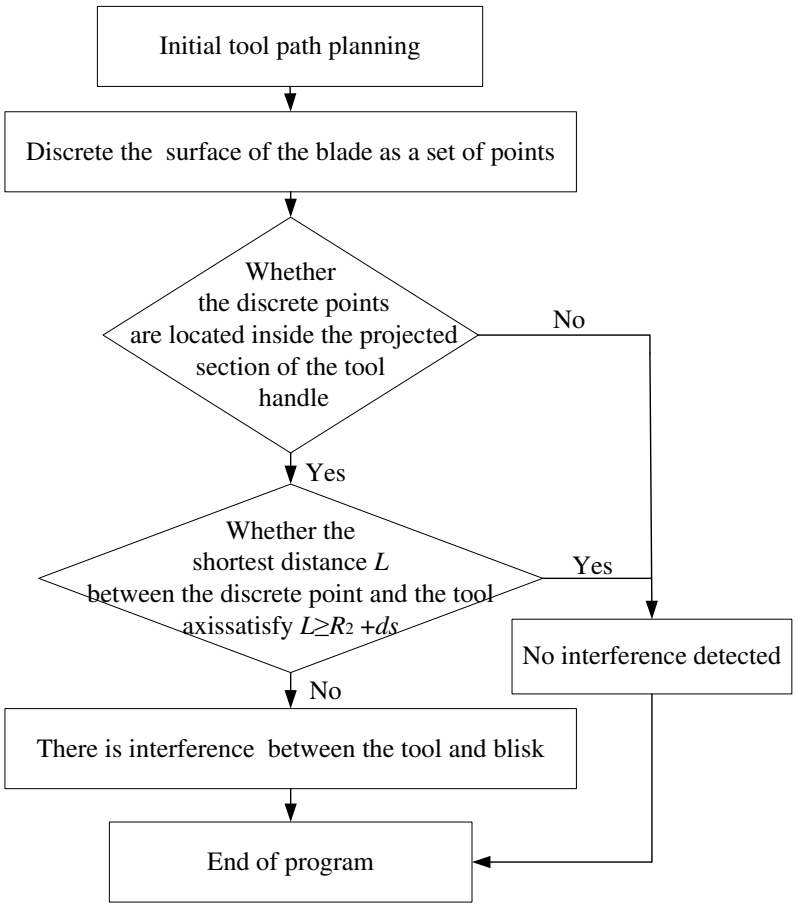

Fig 5 Flow chart of the proposed collision detection method

3. Collision avoidance method

3.1 Collision avoidance when the tool interferes with the polishing blade

At the tool location point $\boldsymbol{P}$ where collision occurs between the tool and the polishing blade, all discrete points in the projected section of the tool handle are traversed to calculate the shortest distance L_a between the tool axis and the discrete points that have interference with the tool. By noting the coordinates of the discrete point corresponding to the shortest distance as $\boldsymbol{F}_a$, the projected coordinate $\boldsymbol{F}_a'$ on the tool axis is

$$\boldsymbol{F}_a' = \boldsymbol{P} + \overrightarrow{\boldsymbol{PF}_a} \cdot \boldsymbol{T} \tag{10}$$

where $\boldsymbol{T}$ is unit vector of the tool axis.

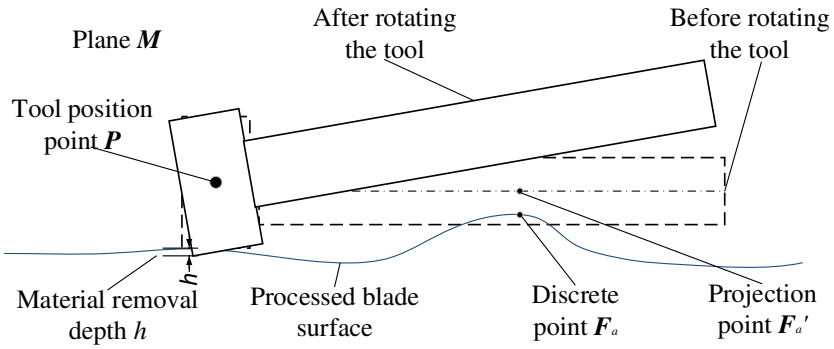

Fig 6 Adjustment of the tool attitude

As shown in Fig 6, in the plane $\boldsymbol{M}$ where the tool position point $\boldsymbol{P}$, the discrete point $\boldsymbol{F}_a$ and its projection point $\boldsymbol{F}_a'$ are located, the tool position point $\boldsymbol{P}$ is used as the fulcrum to rotate the tool until the distance L from the discrete point to the tool axis satisfies the following formula.

$$L=R_2+d \tag{11}$$

where ds is the safe distance between the tool and the blisk.

The tool can be adjusted to a safe orientation with the minimum rotation angle θ when rotating the tool in the plane $\boldsymbol{M}$. The minimum rotation angle of the tool axis is calculated by the following formula.

$$\theta = \arcsin\frac{R_2+ds}{\left\|\overrightarrow{\boldsymbol{PF}_a}\right\|}-\alpha \tag{12}$$

The change of the tool posture has the least impact for the blade surface machining quality when rotating the tool shaft with the minimum rotation angle θ.The new interference-free tool axis vector $\boldsymbol{T}'(t_x',t_y',t_z')$ after collision avoidance is

$$\boldsymbol{T}' = \frac{\overrightarrow{\boldsymbol{PF}_a'}+\dfrac{\overrightarrow{\boldsymbol{F}_a\boldsymbol{F}_a'}}{\left\|\overrightarrow{\boldsymbol{F}_a\boldsymbol{F}_a'}\right\|}\left\|\overrightarrow{\boldsymbol{PF}_a'}\right\|\tan\theta}{\overrightarrow{\boldsymbol{PF}_a'}+\dfrac{\overrightarrow{\boldsymbol{F}_j\boldsymbol{F}_j'}}{\left\|\overrightarrow{\boldsymbol{F}_a\boldsymbol{F}_a'}\right\|}\left\|\overrightarrow{\boldsymbol{PF}_a'}\right\|\tan\theta} \tag{13}$$

Changing the tool axis vector will change the bonding state of the tool's grinding head and the blade surface, which causes excessive polishing and affect the surface quality of the workpiece. Therefore, further processing is required to meet the machining accuracy requirement. Whether the machining accuracy meets the requirement is checked by calculating the material removal depth h of the blade surface after rotating the tool.

$$h \approx \sqrt{(L_1/2)^2+R_1^2}\times\cos(\arctan\frac{L_1}{2R_1}-\theta)-R_1<\varepsilon \tag{14}$$

where L_1 is the width of the polishing head, R_1 is the radius of the polishing tool head, h is the ma-

terial removal depth of the blade's surface after machining, and ε is the error constraint value.

If the material removal depth does not meet the requirement of machining accuracy, the tool needs to move a certain distance along the normal vector of the tool contact point to satisfy the requirement. After that, the tool axis vector remains unchanged, and the new tool position point $\boldsymbol{P}'$ is calculated by the following formula.

$$\boldsymbol{P}'=\boldsymbol{P}+h\times\boldsymbol{N} \tag{15}$$

where $\boldsymbol{P}'$ is the final interference-free tool position, $\boldsymbol{N}(n_x, n_y, n_z)$ is the normal vector at the tool contact point, and the material removal depth h is the translation distance along the normal vector.

The flow chart of the proposed collision avoidance method in this section is summarized in Fig 7.

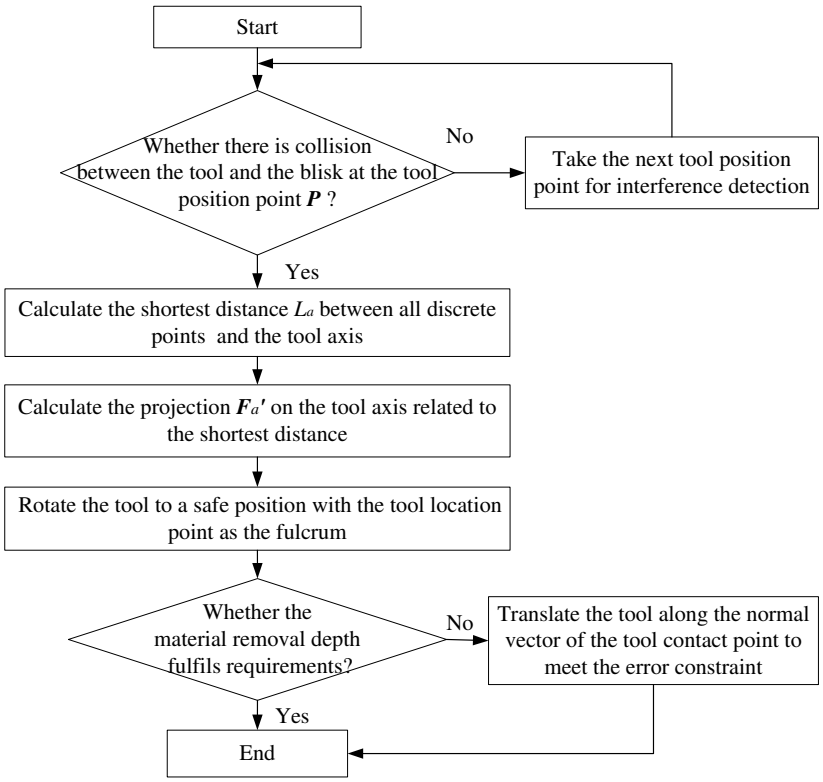

Fig 7 Flow chart of the proposed collision avoidance method

3.2 Collision avoidance treatment when the tool interferes with the adjacent blade

If interference occurs between the tool and the adjacent blade, the tool rotation angle is calculated according to Eq. (11) and Eq. (12), and then the tool is lifted according to Eq. (14) and Eq. (15). The lifting direction is opposite to the rotating direction relative to the polishing blade surface. The tool may interfere with the blisk after being lifted. Therefore, it is necessary to perform iterative calculation. The collision avoidance processing operation should be performed iteratively until non-interference occurs between the tool and the adjacent blade after rotating and lifting the tool. The distance between the discrete point $\boldsymbol{F}_a$ and the tool axis is

$$L_j = R_2 + j \times ds \tag{16}$$

where j is the number of collision avoidance cycles, ds is the safe distance between the tool and the blisk, and R_2 is the radius of the tool handle.

The rotation angle of the tool θ is

$$\theta = \arcsin \frac{L_j}{\|\overrightarrow{PF_a}\|} - \alpha \tag{17}$$

The follow-up processing is the same as Section 3.1, therefore details of the mathematical calculations are not repeated here.

4. Simulation and experiment verification

4.1 Simulation

Visual Studio is used to design the simulation environment of the blisk interference-free tool path generation based on the secondary development of NX 12.0. The experiment is divided into three parts, namely initial tool path generation, collision detection and tool posture correction.

Through the secondary development of NX 12.0, the key information such as the normal vector and curvature of the blade surface is extracted, and the tool path is planned on the surface using the isoparametric method to generate the initial tool path as shown in Fig 8 [17].

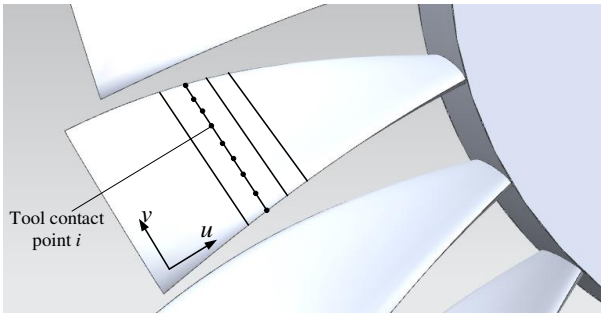

Fig 8 Initial tool path generation

First, interference detection is performed on the initial tool path by using the proposed method in section 2. As shown in Fig.9, two interference situations involving the interference with the polishing blade and the adjacent blade are detected.

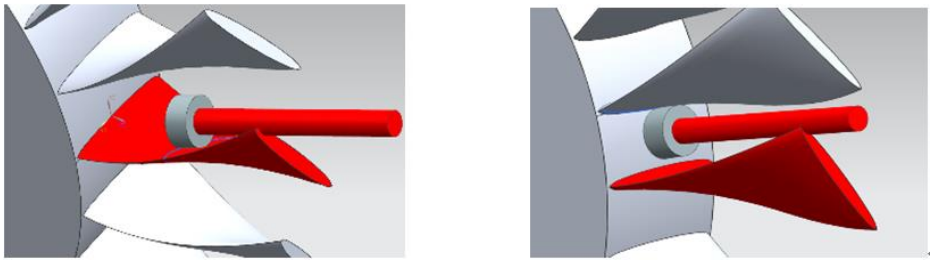

(a) (b)

Fig 9 Interference detection: (a) interference with the polishing blade; (b) interference with the adjacent blade

If the interference is detected, the minimum adjusting angle of the tool is calculated to adjust the

tool to a safe posture by use the proposed method in section 3. Comparisons are performed with the collision avoidance method proposed by Cai [18], which rotate the tool along the normal direction of the interference point to avoid collision. In the tests, there are 22 tool positions that have interference between tool and the polishing blade on one of the tool paths. The rotation angles of the two methods for collision avoidance are shown in Table 1.

Through the comparison, it can be seen that the rotation angles obtained by the proposed method are smaller, which reduces the impact on blade's surface processing quality after changing the tool postures.

After adjusting postures of the tool, the bonding state between the surface of the polishing tool head and the surface of the blade is changed, which causes excessive polishing of the machined surface and affect the processing quality. Taking the above collision points as an example, the material removal depth comparison after rotating the tool posture is shown in Fig 10.

It can be clearly seen from Fig.10 that rotating the tool posture will cause over-polish of the blade surface. The maximum material removal depth can reach 0.308mm, which causes over polishing and affects the processing quality of the blisk seriously. After lifting the tool, the over polishing is eliminated effectively. The distance between the polishing head and the blade surface is controlled within 0mm-0.02mm. The force control mechanism can control the grinding head to fit the blade surface for polishing effectively. Finally, an interference-free tool path that meets the processing requirements is generated. In addition, the tool posture before and after collision avoidance treatment is shown in Fig 11.

Table 1 Rotation angle of the tool attitude adjustment for collision avoidance

Serial number	Rotation angle of the proposed method/[deg]	Rotation angle of Ref.[18]/[deg]
1	2.158	2.711
2	2.345	2.901
3	2.443	3.005
4	2.487	3.054
5	2.527	3.098
6	2.591	3.167
7	2.673	3.252
8	2.767	3.349
9	2.889	3.475
10	3.034	3.623
11	3.166	3.758
12	3.308	3.903
13	3.463	4.060
14	3.626	4.224
15	3.787	4.386
16	3.940	4.539
17	4.127	4.725
18	4.361	4.958
19	4.637	5.233
20	4.763	5.357
21	4.417	5.008
22	3.432	4.019

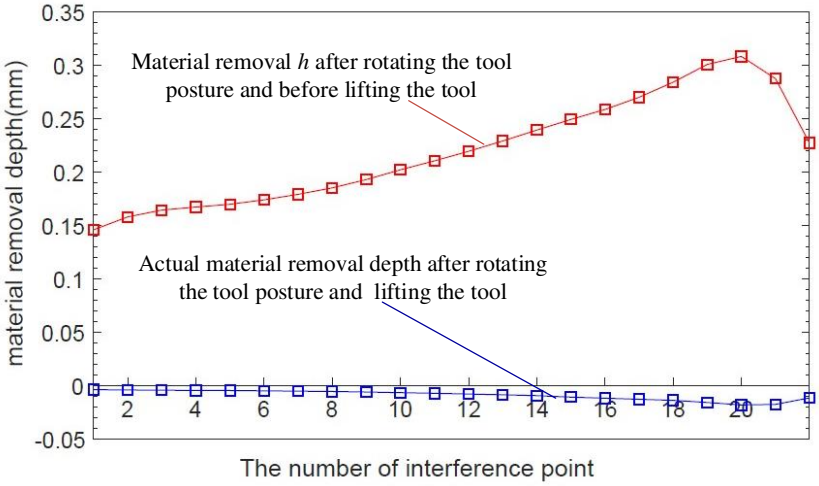

Fig 10 Material removal depth contrast

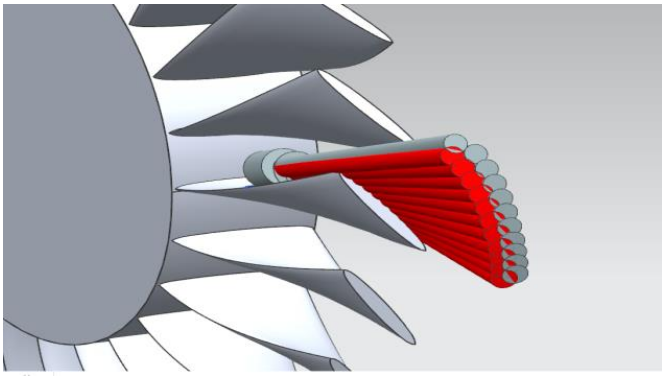

Fig 11 Tool-position correction between the tool and the machined blade

There are seven tool positions that have interference between the tool and the adjacent blade on another tool path. The tool posture before and after collision avoidance is shown in Fig 12.

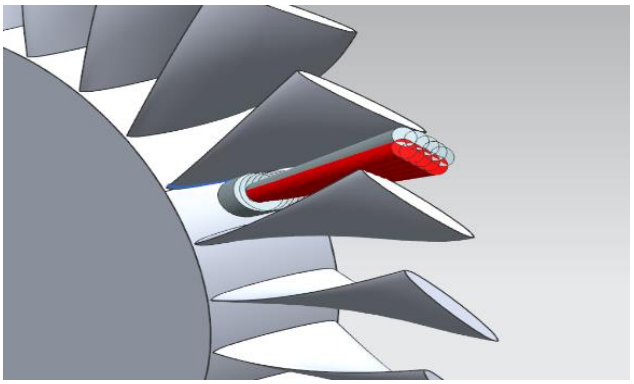

Fig 12 Tool-position correction between the tool and the adjacent blade

The rotation angle, the material removal depth before and after treatment during collision avoidance treatment are shown in Table 2. It can be seen that the material removal depths of generated tool pose satisfy the accuracy requirement after adjusting the tool orientation and position. The

force control mechanism can control the grinding head to fit the blade surface during the polishing process.

Table 2 Tool position correction data in experiments

Serial number	Rotation angle /[deg]	Material removal depth *h* before processing/mm	Actual material removal depth after processing/mm
1	1.703	0.116	-0.004
2	2.689	0.180	-0.009
3	3.065	0.204	-0.013
4	2.968	0.198	-0.011
5	2.651	0.177	-0.008
6	2.247	0.151	-0.005
7	1.735	0.118	-0.002

4.2 Experiment verification

Comau robot is used to perform interference-free polishing experiments of the blisk in this paper. As shown in Fig 13, Comau robot holds the force control mechanism to polish the blisk. Force control polishing is realized by real-time feedback controlling the positive pressure through the force control mechanism.

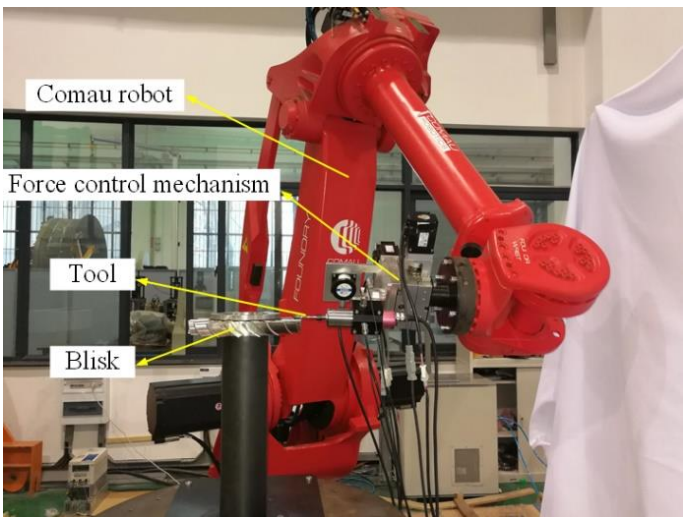

Fig 13 Robot polishing of the blisk

In experiments, the polishing tool path is generated by using the proposed non-interference tool path generation method, and actual polishing tests are conducted on the blisk. As shown in Fig.14, the interference-free polishing of the blisk is effectively realized in the actual machining process.

The blade surface roughness is analyzed to further verify the machining quality of the proposed method. The surface roughness of the blade before and after polishing is shown in Fig.15. It can be seen that the surface roughness of the blade before polishing is 1.406um and the surface roughness of the blade after polishing is 0.358um. The effect of polishing is obvious.

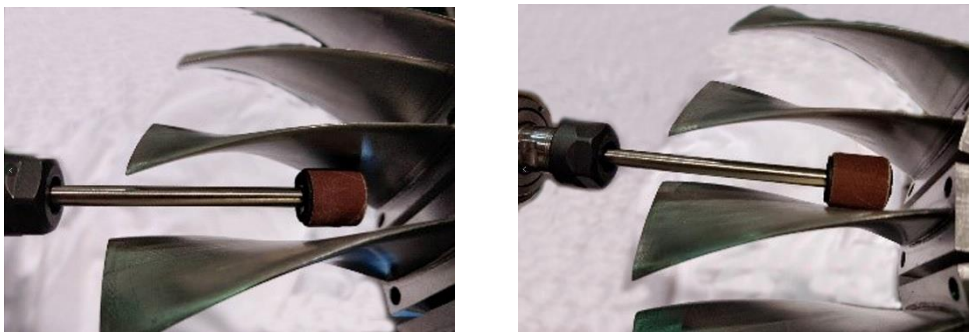

(a)Polishing of the blade convex (b)Polishing of the blade back

Fig 14 Actual polishing of the blisk

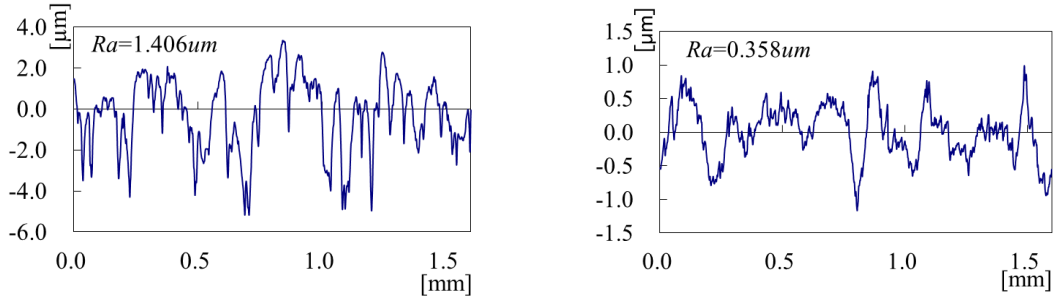

(a) Blade surface roughness before polishing (b) Blade surface roughness after polishing

Fig 15 Blade surface roughness before and after polishing

In summary, it can be seen that the interference-free tool path generation method of the blisk polishing in this paper does not only achieves collision detection and collision avoidance, but also ensures the machining quality of workpiece surface.

5. Conclusions

In order to address the problem of the interference in the polishing process of the blisk，this paper proposes an interference-free tool path generation method of the blisk polishing. The main conclusions are as follows:

(1) The distance between the discrete points on the surface of the blade and the axis of the tool is used to determine whether the tool and the blisk have collision, which improves the efficiency of collision detection.

(2) If the collision is detected, the tool axial vector is adjusted through the minimum rotation angle to avoid collision, which reduces the impact on blade's surface quality after changing the tool postures.

(3) The tool posture after collision avoidance is further adjusted in order to control the material removal depth within the preset limitations, which ensures the quality of workpiece surface.

Simulation and experiments verify that the proposed method realizes the collision detection and avoidance of the blisk polishing effectively. The surface quality of the workpiece is also guaranteed after adjusting the tool posture to avoid interference.

Acknowledgements

This research is supported by the Key Research and Development Plan under Grant No.2020YFB1710400, the National Natural Science Foundation of China (NSFC) under Grant No. 51535004, and the Fundamental Research Funds for the Central Universities under Grant No. 2020kfyXJJS064.

Declarations

-Ethical Approval (Not applicable)

-Consent to Participate (Not applicable)

-Consent to Publish: The authors agree to publication in The International Journal of Advanced Manufacturing Technology.

-Authors Contributions: Yuanming Wang: Conceptualization, Writing - Original Draft, Validation; **Jixiang Yang:** Resources, Instruct, Review; **Dingwei Li:** Experiments; **Han Ding:** Instruct, Review.

-Funding: This research is supported by the Key Research and Development Plan under Grant No.2020YFB1710400, the National Natural Science Foundation of China (NSFC) under Grant No. 51535004, and the Fundamental Research Funds for the Central Universities under Grant No. 2020kfyXJJS064.

-Competing Interests: The authors declare that they have no known competing financial interests or personal relationships that could have appeared to influence the work reported in this paper.

-Availability of data and materials (Not applicable**)**

References

[1] G.J. Xiao, Y. Huang. Equivalent self-adaptive belt grinding for the real-R edge of an aero-engine precision-forged blade[J]. The International Journal of Advanced Manufacturing Technology. 2016, 83(9/12): 1697-1706.

[2] J.H. Duan, Y.Y. Shi, X.J Lin, T. Dong. Flexible Polishing Machine with Dual Grinding Heads for Aeroengine Blade and Blisk[J]. Advanced Materials Research. 2011, 1380.

[3] G.J. Xiao, Y. Huang, J. Wang. Path planning method for longitudinal micromarks on blisk root-fillet with belt grinding[J]. International Journal of Advanced Manufacturing Technology. 2018, 95(1):797-810.

[4] T. Zhang, J. Su. Collision-free planning algorithm of motion path for the robot belt grinding system[J]. International Journal of Advanced Robotic Systems. 2018, 15(4).

[5] C. Ahmet, N. Ali. A novel iso-scallop tool-path generation for efficient five-axis machining of free-form surfaces[J]. The International Journal of Advanced Manufacturing Technology. 2010, 51(9/12): 1083-1098.

[6] T. Lin, J. Lee, E. Bohez. A new accurate curvature matching and optimal tool based five-axis machining algorithm[J]. Journal of Mechanical Science and Technology. 2009, 23(10): 2624-2634.

[7] M.J.B. Fard, H. Feng. Effect of tool tilt angle on machining strip width in five-axis flat-end milling of free-form surfaces[J]. The International Journal of Advanced Manufacturing Technology. 2009, 44(3/4): 211-222.

[8] J. Du, P.C. Liu, H.Y. Zhi, P. Ding. Global interference detection technology for five-axis machining of complex surfaces[J]. The International Journal of Advanced Manufacturing Technology. 2019, 102(9/12): 4273-4287.

[9] Z.W. Wang, X. Lin, Y.Y. Shi. Efficiently constructing collision-free regions of tool orientations for holder in five-axis machining of blisk[J]. Chinese Journal of Aeronautics. 2020, 33(10): 2743-2756.

[10] O. Llushin, G. Elber, D. Halperin, et al. Precise global collision detection in multi-axis NC-machining[J]. Computer-Aided Design. 2004, 37(9).

[11] Z. Huang, P.X. Wei, et.al. Collision detection method for grinding and polishing of blisk [J]. Computer Integrated Manufacturing Systems.: 1-17. (In Chinese)

[12] J.S. Hwang. Interference-free tool-path generation in the NC machining of parametric compound surfaces[J]. Hwang J.S. 1992, 24(12).

[13] S. Ding, M. A Mannan, A. N Poo, et al. Adaptive iso-planar tool path generation for machining of free-form surfaces[J]. Computer-Aided Design. 2003, 35(2).

[14] H. Li, H.Y. Feng. Efficient five-axis machining of free-form surfaces with constant scallop height tool paths[J]. International Journal of Production Research. 2004, 42(12).

[15] C. Tournier. E. Duc. Iso-scallop tool path generation in 5-axis milling[J]. The International Journal of Advanced Manufacturing Technology. 2005, 25(9/10): 867-875.

[16] Y. Takeuchi, K. Morishige, K. Kase. Tool path generation using C-Space for 5-Axis control machining[J]. Journal of manufacturing science and engineering: Transactions of the ASME. 1999, 121(1): 144-149.

[17] Z.X. Gao. Application on Programming and Simulation of the Fan Blade NC Machining Based on UG[J]. Applied Mechanics and Materials. 2015, 3822.

[18] Y.L. Cai, G Xi. Global tool interference detection in five-axis machining of sculptured surfaces. Proceedings of the Institution of Mechanical Engineers, Part B: Journal of Engineering Manufacture. 2002;216(10):1345-1353.

Figures

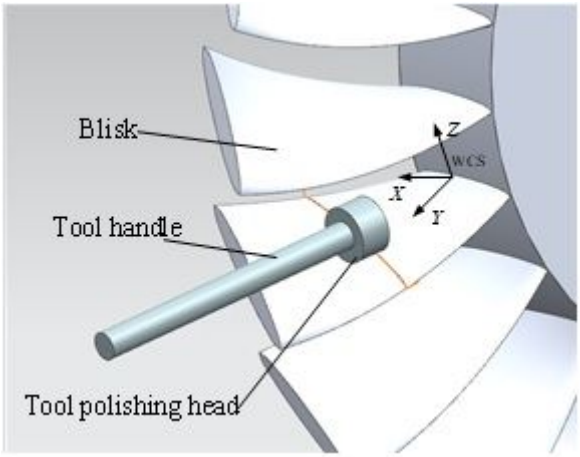

Figure 1

The diagram of blisk polishing

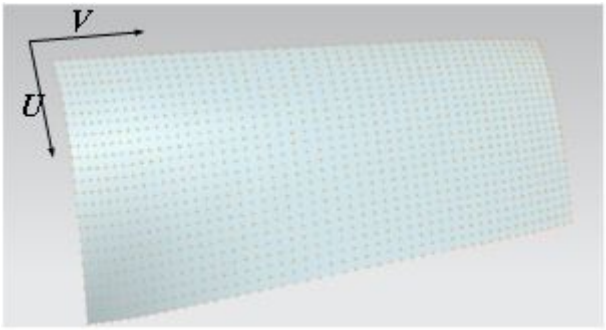

Figure 2

Isometric discretization of blade surface

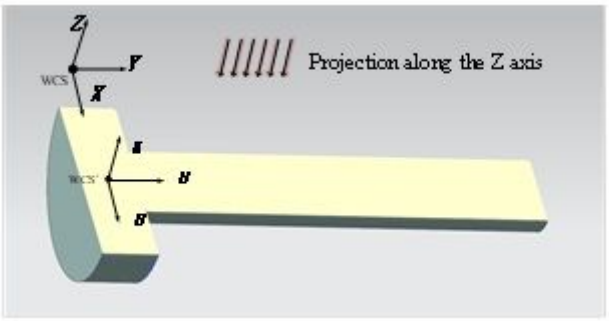

Figure 3

The tool is projected along the negative Z axis

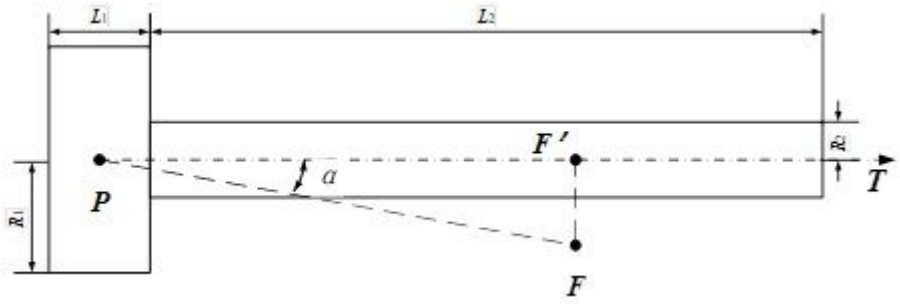

Figure 4

Discrete point and tool surface collision detection

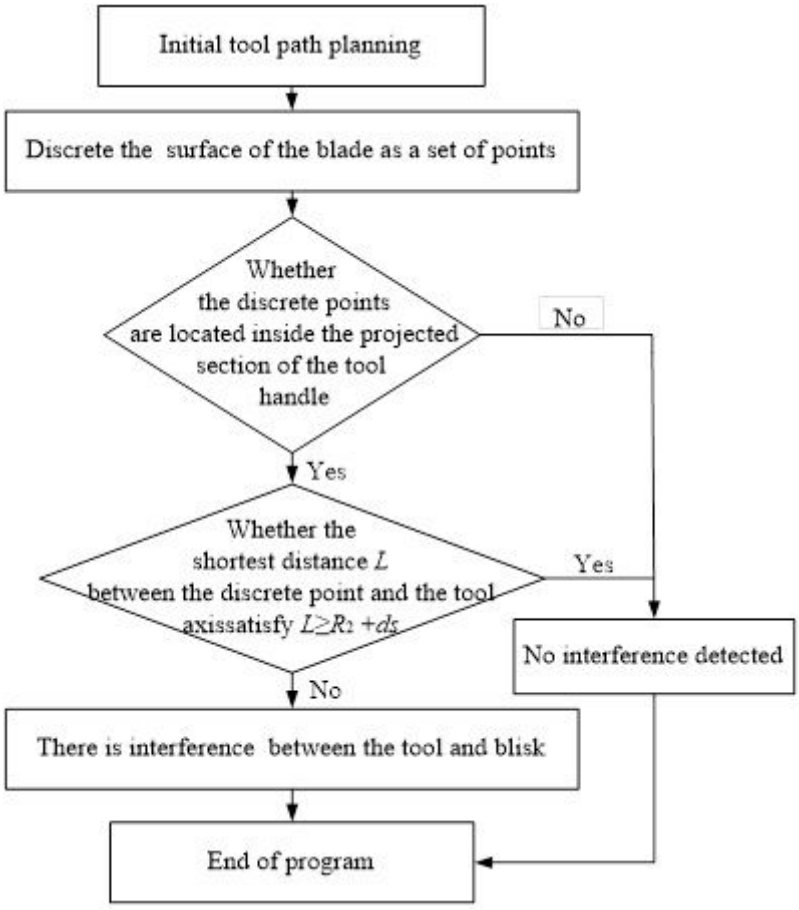

Figure 5

Flow chart of the proposed collision detection method

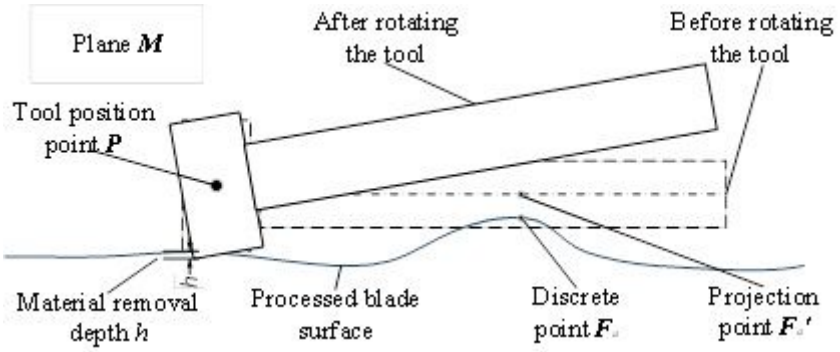

Figure 6

Adjustment of the tool attitude

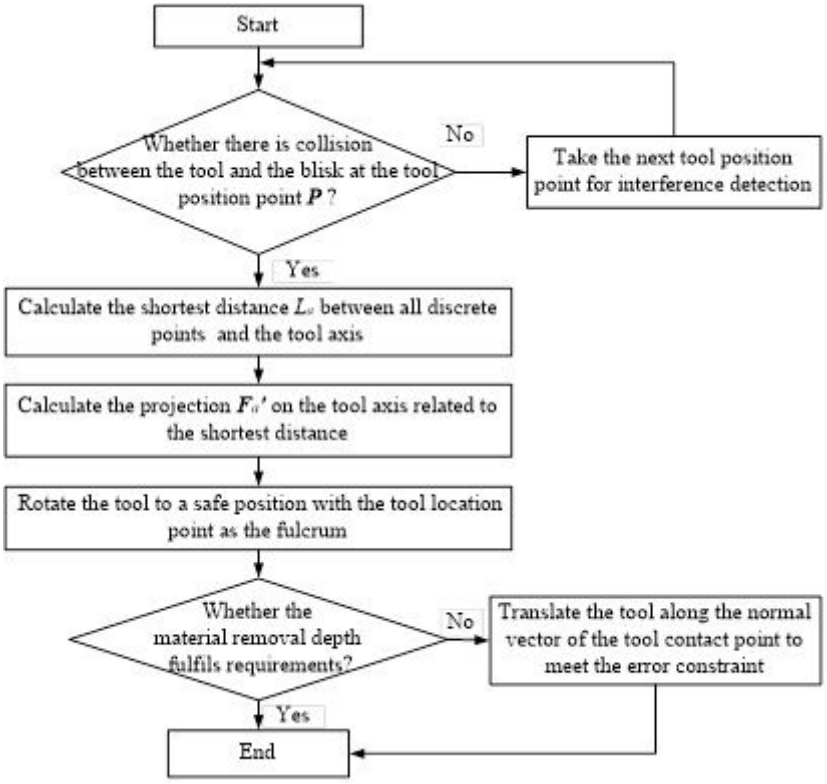

Figure 7

Flow chart of the proposed collision avoidance method

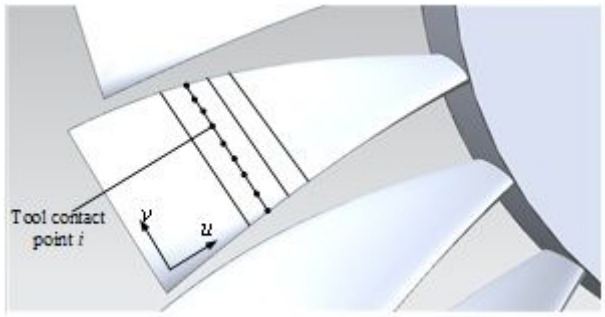

Figure 8

Initial tool path generation

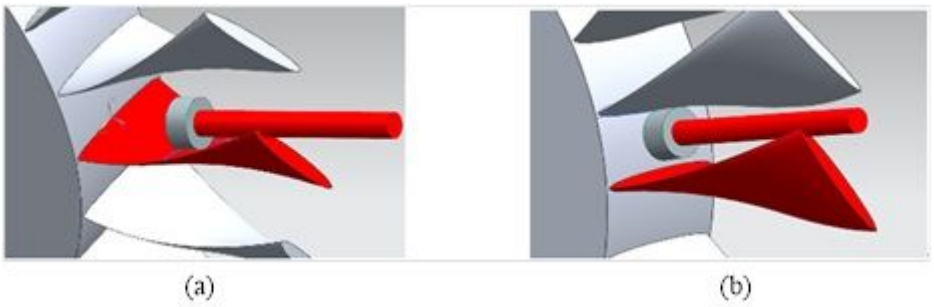

Figure 9

Interference detection: (a) interference with the polishing blade; (b) interference with the adjacent blade

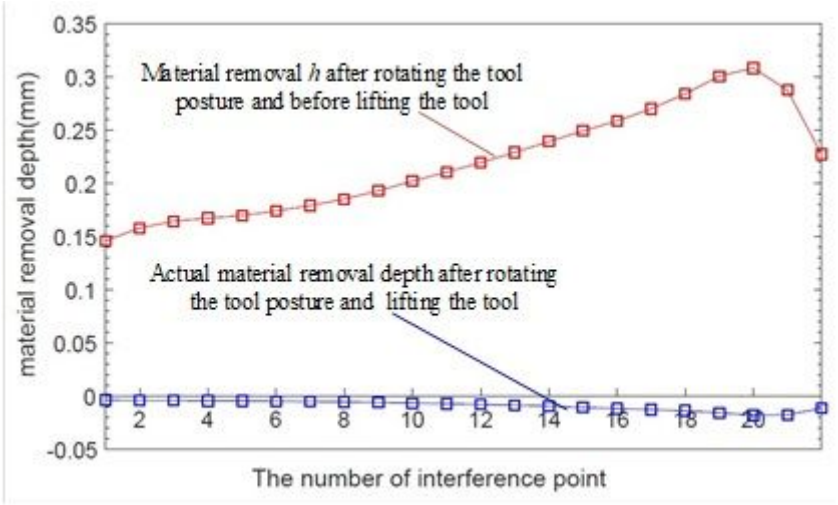

Figure 10

Material removal depth contrast

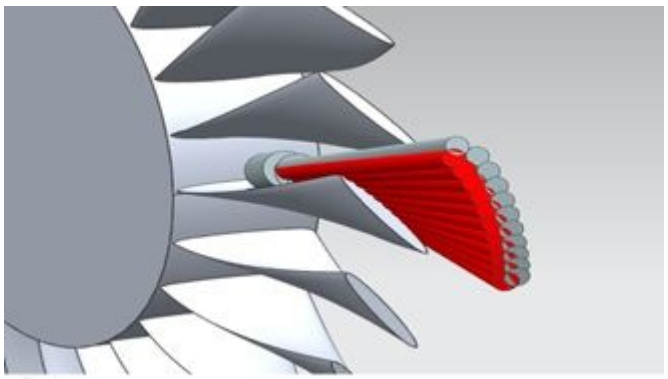

Figure 11

Tool-position correction between the tool and the machined blade

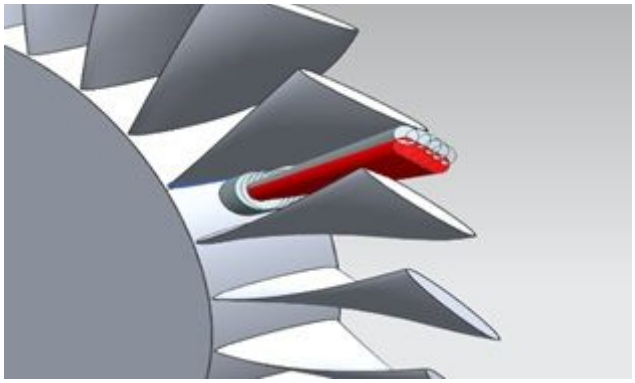

Figure 12

Tool-position correction between the tool and the adjacent blade

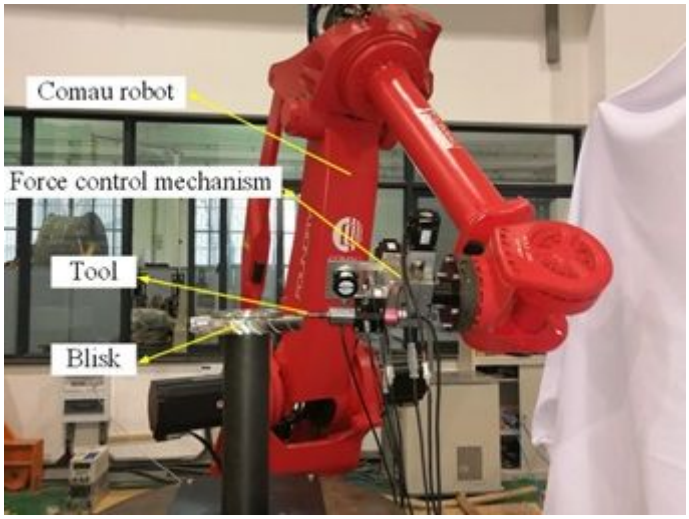

Figure 13

Robot polishing of the blisk

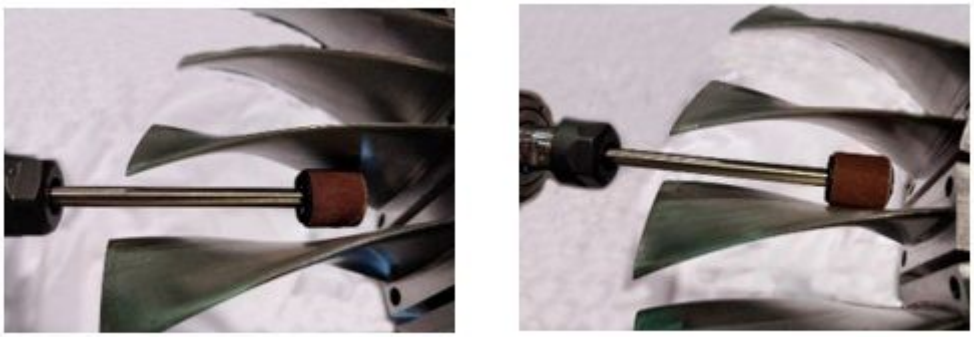

Figure 14

Actual polishing of the blisk

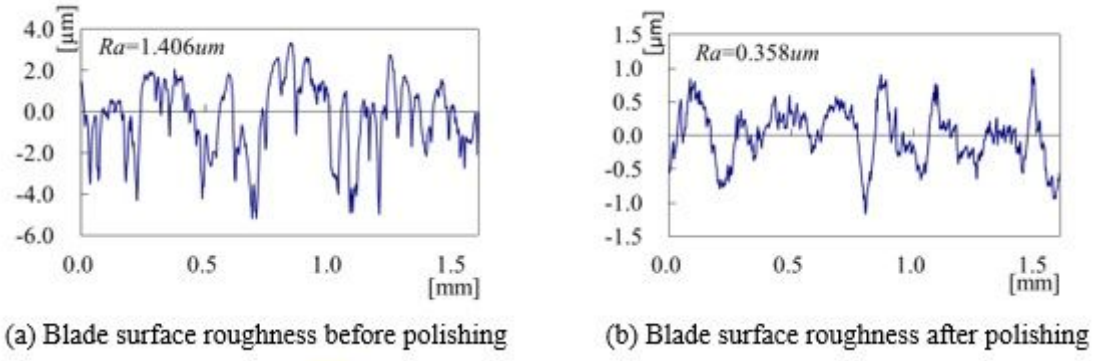

Figure 15

Blade surface roughness before and after polishing